Title

Microstructural properties of premotor pathways predict visuomotor performance in chronic stroke

Journal

Human Brain Mapping, 37(6)

ISSN

1065-9471

Authors

Archer, Derek B
Misra, Gaurav
Patten, Carolynn
et al.

Publication Date

2016-06-01

DOI

10.1002/hbm.23155

Peer reviewed

◆ Human Brain Mapping 37:2039–2054 (2016) ◆

Microstructural Properties of Premotor Pathways Predict Visuomotor Performance in Chronic Stroke

Derek B. Archer,[1] Gaurav Misra,[1] Carolynn Patten,[2] and Stephen A. Coombes[1]*

[1]*Laboratory for Rehabilitation Neuroscience, Department of Applied Physiology and Kinesiology, University of Florida, Gainesville, Florida*
[2]*Neural Control of Movement Lab, Department of Physical Therapy, University of Florida and Malcolm-Randall VA Medical Center, Gainesville, Florida*

Abstract: Microstructural properties of the corticospinal tract (CST) descending from the motor cortex predict strength and motor skill in the chronic phase after stroke. Much less is known about the relation between brain microstructure and visuomotor processing after stroke. In this study, individual's poststroke and age-matched controls performed a unimanual force task separately with each hand at three levels of visual gain. We collected diffusion MRI data and used probabilistic tractography algorithms to identify the primary and premotor CSTs. Fractional anisotropy (FA) within each tract was used to predict changes in force variability across different levels of visual gain. Our observations revealed that individuals poststroke reduced force variability with an increase in visual gain, performed the force task with greater variability as compared with controls across all gain levels, and had lower FA in the primary motor and premotor CSTs. Our results also demonstrated that the CST descending from the premotor cortex, rather than the primary motor cortex, best predicted force variability. Together, these findings demonstrate that the microstructural properties of the premotor CST predict visual gain-related changes in force variability in individuals poststroke. *Hum Brain Mapp 37:2039–2054, 2016.*

Key words: chronic stroke; visual gain; corticospinal tract; fractional anisotropy; tractography; diffusion tensor imaging

INTRODUCTION

Neuroimaging evidence points to the integrity of the corticospinal tract (CST) in the prediction of many of the motor deficits experienced by poststroke individuals [Perez and Cohen, 2009; Schulz et al., 2012; Stinear et al., 2007]. Fractional anisotropy (FA) is reduced poststroke in CST regions such as the cerebral peduncle and the posterior limb of the internal capsule (PLIC) [Park et al., 2013; Schaechter et al., 2008], and FA in these regions correlates positively with measures of motor skill, grip strength, and clinical tests of motor function poststroke [Lindenberg et al., 2010, 2012; Schaechter et al., 2008]. These studies have been crucial in advancing our understanding of CST microstructure and motor function poststroke While many

Contract grant sponsor: American Heart Association; Contract grant number: 15GRNT25700431; Contract grant sponsor: James and Esther King Biomedical Research Program, Florida Department of Health; Contract grant number: 3KN01

*Correspondence to: Stephen A. Coombes, Ph.D., University of Florida, Laboratory for Rehabilitation Neuroscience, Department of Applied Physiology and Kinesiology, PO Box 118206, Florida, USA. E-mail: scoombes@ufl.edu

Conflict of Interest: Stephen A. Coombes is cofounder and manager of Neuroimaging Solutions, LLC.

Received for publication 25 September 2015; Revised 26 January 2016; Accepted 14 February 2016.

DOI: 10.1002/hbm.23155

Published online 27 February 2016 in Wiley Online Library (wileyonlinelibrary.com).

previous studies have focused on the CST originating in the primary motor cortex [Bagce et al., 2012], the CST also projects from the premotor cortex, and the premotor cortex plays an important role in motor function following stroke [Johansen-Berg et al., 2002; Plow et al., 2015]. The goal in this study is to determine whether the microstructural properties of the primary motor CST and the premotor CST predict visuomotor control in individuals poststroke.

The primary motor cortex (M1) is often directly altered following stroke, given its intricate connections with the branches of the middle cerebral artery, which is the most commonly damaged artery in stroke [Cramer et al., 2000]. The premotor areas, however, are less likely to be directly affected following stroke because they are supplied by the anterior cerebral artery [Dum and Strick, 1991; Plow et al., 2015]. Premotor areas were thought to be part of the reticulospinal pathways outputting to the axial and proximal muscles, but retrograde labeling in nonhuman primates has demonstrated that 40% of the CST descending to the hand originates from the premotor areas [Dum and Strick, 1991]. Therefore, the CSTs descending from premotor regions could serve as alternatives to the CST descending from M1. The dorsal premotor cortex (PMd) receives visual and somatosensory information from the medial intraparietal area, and is involved in the planning and execution of movement [Kantak et al., 2012]. The ventral premotor cortex (PMv) is engaged during grasping tasks, and receives sensory information from the anterior intraparietal area [Kantak et al., 2012]. These properties of PMd and PMv point to their importance in rehabilitation, as one common characteristic shared by many therapeutic strategies for stroke rehabilitation is performing movement guided by vision [Bagce et al., 2012; Krebs et al., 1998; Patten et al., 2013; Volpe et al., 2000]. Indeed, the premotor areas are key components of the visuomotor network, play a critical role in feedback control [Coombes et al., 2010; Vaillancourt et al., 2006b], and their role in rehabilitation after stroke continues to gain traction [Kantak et al., 2012; Plow et al., 2015]. In nonhuman primates, neuronal activity in premotor cortex increases during the planning phase of arm movements [Hoshi and Tanji, 2000], and perturbing premotor cortex in humans via transcranial magnetic stimulation (TMS) disrupts upper-extremity movement [Mochizuki et al., 2005; Schluter et al., 1998]. Other evidence for involvement of premotor areas in visuomotor control comes from a visual gain experiment in healthy adults, which demonstrated that increases in visual gain led to decreases in force variability and increases in functional activity in PMd and PMv [Coombes et al., 2010]. Hence, premotor areas are more likely to be intact following stroke, play a major role in the planning and execution of movements that are guided by visual feedback, and exhibit increased activity when visuomotor processing demands are increased. Together, these findings lead to the hypothesis that FA of the descending motor pathways projecting from both PMd and PMv may predict visuomotor processing in poststroke individuals, but there is currently no direct evidence that this is the case.

Visuomotor processing can be manipulated by changing visual gain during a force control task [Coombes et al., 2010; Lee Hong and Newell, 2008; Vaillancourt et al., 2006a]. Visual gain is calculated by determining the performance error, in relation to a target, in real-time, and then magnifying or minimizing this error before it is presented to the subject as feedback [Newell and McDonald, 1994]. Increases in visual gain reduce variability in force production in healthy adults [Coombes et al., 2010; Lee Hong and Newell, 2008; Vaillancourt et al., 2006a], and lead to small, but significant improvements in motor control and upper-extremity function in individuals in the chronic phase after stroke [Abdollahi et al., 2013; Patton et al., 2006]. While a recent study shows that baseline measures of CST microstructure predict changes in clinical scores following a two week intervention [Lindenberg et al., 2012], it remains unclear if CST microstructure projecting from M1 alone can predict visual gain induced changes in force performance after stroke, or whether projections from PMd and PMv also contribute.

In this study, individuals poststroke and controls performed a unimanual force task separately with each hand at three levels of visual gain. We collected diffusion MRI from each subject and used probabilistic tractography algorithms to identify the primary and premotor CSTs. Measures of FA within each tract were then used to predict changes in force variability across different levels of visual gain. We tested the hypothesis that parametrically increasing visual gain would improve motor performance (i.e., reduce force variability) in both groups, and that the stroke group would display greater variability at each gain level. Second, in the stroke group, we tested the hypothesis that FA in M1, PMd, and PMv CSTs would predict force performance at each gain level.

METHODS

Subjects

Fourteen individuals poststroke and fourteen healthy control subjects were enrolled. Group demographics and clinical information are shown in Table I. Inclusion criteria for poststroke individuals were as follows: (1) at least six months following a single ischemic stroke affecting motor function in the contralateral hand, (2) able to apply force to a force transducer in the pinch grip configuration, (3) have intact sensation to light touch in the contralateral hand, and (4) able to provide informed consent. Each subject provided informed consent before testing, which was approved by the local Institutional Review Board and was in accord with the Declaration of Helsinki.

TABLE I. Group demographics and relevant clinical information

Subject	Age (yrs)	Sex	Time since stroke (yrs)	Stroke location	Affected hemisphere	FMA motor score	FMA sensation	MAS median	MMSE
1	46	M	4.6	C/SC	L	9	11	2	28
2	63	M	12.4	C/SC	L	49	12	1	27
3	52	M	0.73	SC	L	45	8	1	30
4	79	M	10.21	C/SC	L	62	9	0	29
5	76	F	2.67	SC	L	64	12	0	30
6	56	M	24.45	SC	L	30	7	0	24
7	77	M	12.48	C	L	10	12	0	27
8	59	M	17.65	C/SC	L	51	12	0	27
9	65	M	5.59	SC	L	28	12	3	29
10	56	M	4.3	C/SC	R	30	4	0	30
11	57	M	9.61	C	R	26	10	1	30
12	67	F	1.52	C	R	62	12	1	30
13	31	M	5.53	C	R	19	10	3	29.5
14	75	F	4.67	SC	R	30	12	1	27
Mean	**61.36 ± 13.39**	**11M/3F**	**8.32 ± 6.69**		**9L/5R**	**36.79 ± 18.75**	**10.20 ± 2.5**	**0.9 ±1.1**	**28.39 ± 1.80**
Control	**56.57 ± 10.45**	**10M/4F**				**n/a**	**n/a**	**n/a**	**29.9 ± 0.27**

Mean values are reported ± standard deviation. Abbreviations: yrs, years; M, Male; F, Female; L, Left; R, Right; C, Cortical Stroke; SC, Subcortical Stroke; FMA, Fugl-Meyer Assessment; MAS, Modified Ashworth Scale; MMSE, Mini-Mental State Exam. The motor (66 points) and sensory (12 points) portions of the upper-extremity FMA are reported. MAS scores are reported as median of: shoulder flexion, abduction, external rotation; elbow flexion, extension; wrist flexion, extension, by individual. Lesion conjunction is illustrated in Figure 2.

Clinical Evaluations

Motor impairments of the upper extremities of stroke subjects were assessed with the upper-extremity section of the Fugl-Meyer Assessment (UE FMA) [Fugl-Meyer et al., 1975; Gladstone et al., 2002]. Hemiparetic severity (mean UE FMA 36.8/66 points) and stroke chronicity (mean 8.4 years) captured a wide range of representative individuals with upper-extremity motor impairments following stroke. Age was not significantly different between groups [$t(26) = 1.05$; $P = 0.30$] and control subjects (range 31–74 years) were well matched to the individuals poststroke (range 31–79) for both age and sex. Healthy control subjects were not evaluated with the UE FMA due to its well-recognized ceiling effect, even among individuals poststroke (i.e., maximum score of 66 points does not represent normal or unimpaired motor function). Hypertonicity was measured using the Modified Ashworth Scale [Bohannon and Smith, 1987; Haas et al., 1996]. Cognitive status was screened using the Mini-Mental State Examination [Folstein et al., 1975]. Stroke subjects self-reported pre-morbid hand dominance. Hand dominance in controls was determined using the Edinburgh Handedness Inventory [Oldfield, 1971].

Force Data Acquisition

Subjects laid in the supine position, with their forearms resting on their lower trunk and one force transducer held in each hand at all times. Subjects produced force against a custom fiber-optic force transducer with a resolution of 0.025 N (Neuroimaging Solutions LLC, Gainesville, FL). The force produced by the subject was transmitted via fiber-optic cable to a SM130 Optical Sensing Interrogator (Micron Optics, Atlanta, Georgia). The interrogator digitized the analog force data at 125 Hz. Customized software written in LabVIEW (National Instruments, Austin, TX) collected the force data and then converted the data to Newtons (N). The output from the force transducer was presented to the subject using a visual display at a refresh rate of 60 Hz. Force data were low-pass filtered before analysis (Butterworth, 20 Hz fourth-order dual-pass).

Force Task

Each subject's maximum voluntary contraction (MVC) was measured from each hand during a practice session. Subjects were asked to maintain a contraction of maximum force for three consecutive 5 s trials. Each trial was separated by a 60 s period of rest. The MVC was calculated as the average force during the sustained maximum force contraction. During the task, subjects produced unimanual force to a target force of 15% of their MVC by gripping the force transducer between their thumb and index finger (Fig. 1A). Blocks of trials were performed unimanually with the impaired and less-impaired hand for stroke subjects, and the dominant and nondominant hand for controls. Herein, the impaired hand of the stroke group and

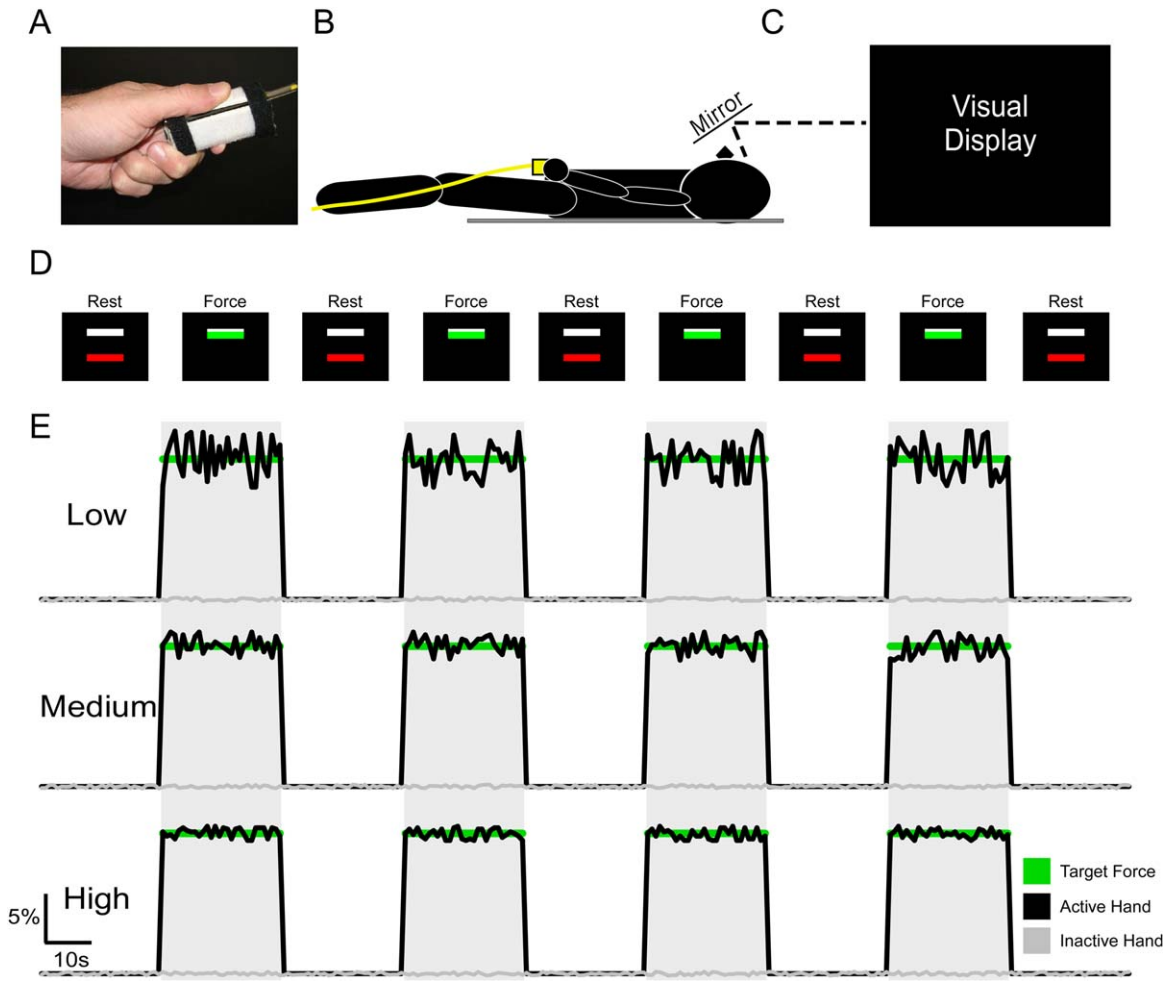

Figure 1.

Experimental Setup. The force transducer was held between the thumb and the index finger by the subject during the MRI session (**A**), and the subject laid in the supine position in which the hand and transducer rested at the lower trunk (**B**). Above the field of view of the subject was a mirror, which reflected the visual display (**C**). The visual display instructed the subject when to produce force. The subject initially saw two bars (one red, one white) on the black screen, which indicated the "Rest" condition. The white bar was set at 15% of each subject's MVC. Following the 30 s Rest condition, the red bar would turn green which indicated the "Force" condition. Subjects were instructed, which hand to use before the task began, and to produce no force with their other hand. During the force condition, the goal was to produce 15% MVC, which would cover the white bar so that it was not visible. Following the Force condition, the trial was repeated. This was repeated four times for each gain level, and for each hand. **E**: Example data is shown for each gain level. Force data corresponds with the visual display instructions shown in D. The green line represents 15% MVC, the black line represents force data for the hand used in the task, and the gray line represents force data for the hand not used in the task.

the nondominant hand of the control group will be referred to as the impaired hand. The less-impaired hand of the stroke and the dominant hand of the control group will be referred to as the unimpaired hand. Three unimanual tasks were completed by each hand: low visual gain, medium visual gain, and high visual gain. Subjects completed a total of six tasks (two hands, three gain levels) while lying in the supine position in the MRI scanner (Fig. 1B).

There were two conditions within each task: Rest and Force. The visual display (Fig. 1C) consisted of two bars, one white, and one red/green as shown in Figure 1D. The white target bar was set at 15% of each subject's MVC. The red/green bar was used to cue the subject to rest or

to produce force. During the Rest condition subjects were instructed to fixate on the red bar. When the bar turned green, the subjects began producing isometric force and the bar fluctuated in real-time to reflect the amount of force being produced. Subjects were instructed to be as accurate as possible and cover the white target bar with the green force bar. Rest and Force conditions each lasted 30 s and were alternated within tasks. Each task began and ended with a Rest period. Blocks within each task followed the same sequence, were displayed on the visual display (Fig. 1D), and lasted 270 s total. The independent variable that was manipulated between scans was visual gain.

Visual Gain

Visual feedback was altered between tasks by changing the visual gain of the real-time feedback. The difference between the amount of force produced by the subject and the target force was calculated. This difference was then multiplied by a visual gain factor (low, medium, high), which manipulated the spatial amplitude of visual feedback by altering the height of force fluctuations on the visual display using the following formula:

$$\text{Cursor Position} = (F_p - F_t) * G + F_t \quad (1)$$

in which F_p is the force produced by the subject, F_t is the target force, and G is the gain level used to manipulate the spatial amplitude of visual feedback.

Based on prior work [Vaillancourt et al., 2006a], we calculated the visual angle for each visual gain level by assuming a set force output standard deviation of 0.3 N. This estimate was derived from previous studies [Laidlaw et al., 2000; Slifkin and Newell, 1999]. The value of the standard deviation was multiplied by 6 to approximate the full range (±3 standard deviations) of estimated variance for the height of the force fluctuations. The visual angle for each gain level was then calculated using the following formula:

$$\propto = 2 * \tan^{-1}\left(\frac{H1}{D}\right) \quad (2)$$

in which α is the visual angle, D is the distance to the display, and $H1$ is the height of the total range of motion in the top half of the visual field. Because previous evidence has shown that performance error approaches an asymptote at ~0.5°, we ensured that low gain was well below 0.5° and that high gain was well above 0.5° [Coombes et al., 2010]. The low, medium, and high visual gain levels corresponded to visual angles of 0.039°, 0.39°, and 2.39°, respectively. The task was performed unimanually by each hand at the low, medium, and high gain level. Example force output is shown in Figure 1E, which shows that low gain resulted in greater fluctuations in force output around the target force level. Increases in visual gain at the medium and high gain levels show a reduction in the fluctuation of force output around the target force level. To control for potential order effects, both hand order and visual gain order for each hand were counterbalanced across subjects.

Force Data Analysis

Force data were analyzed using custom algorithms in LabVIEW. Two measures were calculated: mean force and force variability (standard deviation). Force measures were calculated using an 18 s portion of each contraction starting 7 s after contraction onset and ending 5 s before the end of the contraction. We excluded beginning and end effects of force production as they are likely independent of visuomotor processing [Coombes et al., 2010, 2011; Lodha et al., 2012a, 2012b; Naik et al., 2011]. Mean force and force variability were calculated separately for each hand at each gain level. In addition, an asymmetry value was calculated for each force measure [(unimpaired measure − impaired measure)/(unimpaired measure + impaired measure)]. Lower asymmetry scores reflect greater mean force and greater force variability in the impaired hand.

MRI Acquisition

Magnetic resonance images were collected using a 32 channel head coil inside a 3 Tesla magnetic resonance scanner (Achieva, Best, The Netherlands). T1-weighted images (resolution: 1 mm isotropic, TR = 6.8 ms, TE = 3.3 ms, flip angle = 8°) and diffusion MRI images (resolution: 2 mm isotropic, 64 noncollinear diffusion directions, *b*-value of 1,000 s/mm^2 and one with a *b*-value of 0 s/mm^2, 75 axial slices covered the cortex and brainstem) were collected from each subject.

MRI Preprocessing

Prior to analyses, the diffusion MRI volumes and T1 images of 5 subjects with lesions in the right hemisphere were flipped along the mid-sagittal plane, so that the impaired hemisphere had the same coordinates for all subjects [Lindenberg et al., 2012; Wang et al., 2012]. The lesioned hemisphere in the stroke group and the hemisphere contralateral to the nondominant hand in the control group will be referred to as the impaired hemisphere. The nonlesioned hemisphere in the stroke group and the hemisphere contralateral to the dominant hand in the control group will be referred to as the unimpaired hemisphere. FSL (fsl.fmrib.ox.ac.uk) was used for all diffusion MRI (dMRI) data analyses [Jenkinson et al., 2012; Smith et al., 2004; Woolrich et al., 2009]. The dMRI data were corrected for eddy currents and head motion using a 3-D affine registration, and the brain was extracted [Smith, 2002]. FA values were obtained from the dMRI data. The

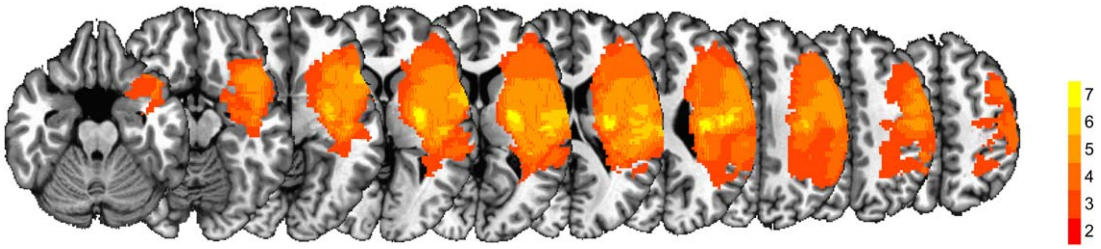

Figure 2.

Lesion Conjunction Map. The lesion conjunction across subjects shown on a series of axial T1 slices. The color bar represents the number of individuals with a lesion in each voxel. Dark colors (red) indicate fewer subjects with a lesion in the same voxel, whereas brighter colors (yellow) indicate higher lesion overlap in the same voxel.

FA map was normalized into standard space using a linear transformation (FLIRT) [Jenkinson and Smith, 2001; Jenkinson et al., 2002] followed by a nonlinear transformation (FNIRT) [Jenkinson et al., 2012; Smith et al., 2004; Woolrich et al., 2009]. Lesions were masked out during both transformations to prevent lesion related distortions and inaccuracies of transformations. Goodness of fit to the standard template was confirmed visually by evaluating the position of the corpus callosum for each subject.

Lesion Characterization

Structural T1-weighted images were transformed using the same dMRI normalization technique outlined above. These images were used to assess lesion characteristics in the stroke group. Lesions were manually drawn on the T1 image by two raters for each stroke subject. Manual lesion drawing is comparable in accuracy to semiautomatic lesion identification [Clas et al., 2012; de Haan et al., 2015; Wilke et al., 2011]. Lesions were then transformed into standard space using the diffusion nonlinear warp field. Inter-rater reliability of manual lesion drawing was examined using intraclass correlation coefficients (ICC) between the two drawers. The ICC was high for all variables, including FA (ICC = 0.81), center of mass (ICC = 0.99, 0.88, and 0.97 for x, y, and z, respectively), and volume (ICC = 0.83). As FA was our variable of interest, we performed t-tests between FA values in each lesion drawn by the two drawers, which did not identify any significant differences [$t(26)=1.3$, $P = 0.20$]. To prevent the effect of lesions within the FA maps from confounding analyses, voxels within the lesion were excluded from all FA analyses. Figure 2 shows the lesion conjunction map for all stroke subjects throughout the whole brain. The maximum overlap within the entire brain did not exceed 7/14, and the maximum overlap occurred within the external capsule at $x = -31$, $y = -3$, $z = -1$.

Probabilistic Tractography

Probabilistic tractography was conducted to identify primary and premotor CST projections. First, a probability distribution was estimated for each voxel modelling all possible fiber directions by using the eddy current corrected images. To identify both the primary and premotor CSTs, the cerebral peduncle was used as a seed (obtained from Johns Hopkins University white-matter labels atlas). Next, waypoints were selected to partition each tract appropriately: a spherical mask of 8mm was placed in M1 at $x = 24$, $y = -28$, and $z = 53$ to identify the primary CST projections, and spherical masks of 8mm diameter were placed in PMd at $x = 33$, $y = -7$, and $z = 51$, and PMv at $x = 53$, $y = 2$, and $z = 36$ to identify the secondary CST projections [Coombes et al., 2010]. To obtain specific tracts, one mask was used as a waypoint while the other masks were used as exclusion masks. For instance, when identifying the CST projections between the cerebral peduncle and PMv, spheres in M1 and PMd were used as exclusion masks. An exclusion mask was also placed at the midline to eliminate transcallosal fibers.

In addition to the motor tracts, we used probabilistic tractography to track the ventral and dorsal visual streams, as previous studies have also associated these tracts with visuomotor processing [Caeyenberghs et al., 2010; Jager, 2005; Wolter and Preda, 2006; Yoshida et al., 2010]. To identify the ventral stream, the primary visual cortex (V1) ($x = 20.9$, $y = -57.9$, $z = -6.1$) was used as a seed [Haar et al., 2015]. Waypoints for the ventral stream were a planar waypoint, which was placed inferior to V1 ($z = -11$), and an additional axial planar waypoint that was placed at the level of the fusiform gyrus ($z = -19$). A planar exclusion mask was placed superior to V1 to exclude dorsal stream fibers ($z = -2$). The dorsal stream was identified by placing a seed in the superior longitudinal fasciculus, and a 8 mm sphere in the extrastriate visual area (V3) ($x = -43.8$, $y = -68$, $z = -5.7$) was used as a waypoint [Coombes et al., 2010]. A midline exclusion mask ($x = 0$) was used to exclude any transcallosal connections for both tracts, and the thalamus was used as an exclusion mask to exclude any connections to the primary visual pathway.

Tracking was performed with default parameters (number of samples = 5,000, curvature threshold = 0.2,

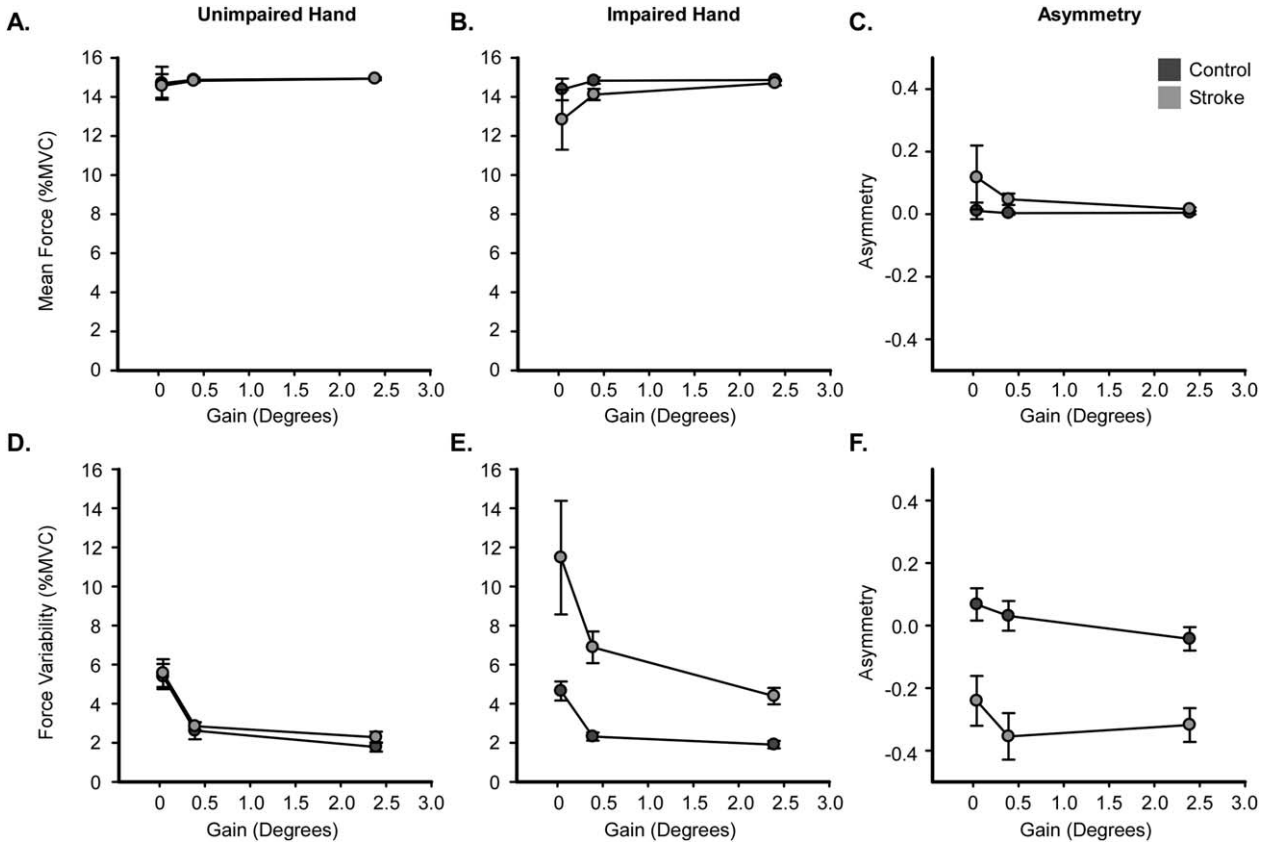

Figure 3.

Force Amplitude and Force Variability. Mean force amplitude is shown for the unimpaired (**A**) and impaired hand (**B**) for both the control (dark gray) and stroke (light gray) groups. **C**: shows the asymmetry of mean force amplitude for both groups. Force variability is shown for the unimpaired (**D**) and impaired hand (**E**) for both groups. Corresponding asymmetry values are shown in **F**. Each data point represents the group mean at each level of visual gain, and error bars represent ± SEM.

minimum FA = 0.2). Tracking results were then thresholded so that only the top 5% of probable voxels was included. For each tract, a group template were calculated in standard space by overlaying tracts from all control subjects to build a conjunction map. Areas of each tract with high overlap between subjects were binarized to create a group level template for each tract. Region specific differences of FA in each group level tract template were calculated using a slice-by-slice approach, which allowed us to determine mean FA in each slice of the tract along its primary axis of travel for each individual. A custom linux shell-script computed the average FA of the tract for each individual at each slice. We then compared the average FA within each slice between groups by conducting FDR corrected independent samples t-test.

An average FA profile was then calculated for each group for each hemisphere. FA asymmetry profiles were created by calculating the asymmetry at each slice for each tract [(unimpaired tract FA – impaired tract FA)/(unimpaired tract FA + impaired tract FA)]. This asymmetry approach controls for within subject variability in FA, and is consistent with studies that have associated FA asymmetry with behavioral measures [Lindenberg et al., 2010; Park et al., 2013; Stinear et al., 2007; Wang et al., 2012]. Higher asymmetry scores indicate lower FA in the impaired hemisphere compared to the unimpaired hemisphere. Asymmetry scores were compared between groups at each slice using FDR corrected independent samples t-test.

Regression Analyses

For each tract, a region of interest (ROI) was created by evaluating the FA asymmetry profile. Each ROI included three slices. The slice, which contained the highest asymmetry value, was used as the center of the ROI. For the motor tracts, a slice superior to the center and a slice inferior to the center were also used in the ROI. For the visual

TABLE II. Mean force amplitude and force variability

	Low gain				Medium gain				High gain			
	Control		Stroke		Control		Stroke		Control		Stroke	
	Mean	SD	Mean	SD	Mean	SD	Mean	SD	Mean	SD	Mean	SD
Force (%MVC)												
Unimpaired	14.70	3.15	14.56	2.27	14.87	0.44	14.82	0.30	14.94	0.34	14.93	0.14
Impaired	14.38	2.07	12.83	5.74	14.83	0.60	14.12	1.09	14.86	0.10	14.70	0.41
Asymmetry	0.01	0.10	0.12	0.38	0.00	0.02	0.05	0.07	0.00	0.02	0.02	0.02
Variability (% MVC)												
Unimpaired	5.39	2.41	5.57	2.65	2.62	1.65	2.85	0.74	1.79	0.89	2.28	1.07
Impaired	4.65	1.81	11.48	10.87	2.32	0.78	6.89	3.02	1.90	0.72	4.39	1.57
Asymmetry	0.07	0.19	−0.24	0.30	0.03	0.18	−0.35	0.28	−0.04	0.14	−0.32	0.20

Mean and standard deviation values are shown for the unimpaired hand, impaired hand, and asymmetry for both mean force amplitude and mean force variability.

tracts, a slice posterior to the center and anterior to the center were included in the ROI. FA within each ROI (M1, PMd, PMv, ventral, dorsal), subject age, lesion age, lesion size, and UE FMA were used as independent variables in a multivariate multiple regression analysis to predict the variables (force amplitude and/or force variability) with significant differences between groups, at each gain level. A bidirectional stepwise regression analysis was used to determine which independent variables best described variance in the dependent variables. The model with the highest R^2_{adj} was selected as the best fit model, and the contribution of each independent variable to this best fit model was calculated [Gromping, 2006]. Significant multivariate multiple regression analyses were followed up with multiple regression analyses to determine the contribution of each independent variable at each level of visual gain. Statistical analyses were performed using the R statistical analysis package (Version 3.0.2, www.r-project.org).

RESULTS

Maximum Voluntary Contraction

The average MVC of the impaired hand for the stroke group (36.44 ± 5.66 N) was significantly less [$t(26) = 4.22$; $P < 0.001$] than the average MVC of the impaired hand for the control group (73.11 ± 6.60 N). The average MVC of the unimpaired hand for the stroke group (70.19 ± 5.40 N) was not significantly different than the average MVC of the unimpaired hand for the control group (79.33 ± 6.95 N).

Force Data Analysis

Force amplitude

Mean force produced by the unimpaired hand is shown in Figure 3A and the impaired hand in Figure 3B. Mean force across all task conditions and groups ranged from 12.83 to 14.86% MVC. Consistent with the data shown in Figure 3A, the group × gain ANOVA model to assess mean force produced by the unimpaired hand revealed no significant effect of group [$F(1,26) = 0.03$; $P = 0.88$], gain [$F(1.01,26.22) = 0.33$; $P = 0.57$], or group × gain interaction [$F(1.01, 26.22) = 0.02$; $P = 0.90$]. As shown in Figure 3B, mean force produced by the impaired hand at the low gain level for the stroke group was 12.83% MVC and 14.38% MVC for the control group, respectively. At medium and high gain levels, mean force was within 1% of the target force level for both groups. Similar to findings in the nonimpaired hand, the two-way [group (2) × gain (3)] ANOVA of mean force for the impaired hand revealed no significant effect of gain [$F(1.05,27.25) = 1.79$; $P = 0.19$], group [$F(1,26) = 1.75$; $P = 0.20$], or group × gain interaction [$F(1.05,27.25) = 0.58$; $P = 0.46$]. Consistent with these findings, Figure 3C shows asymmetry scores for mean force, and shows that there was no group effect, gain effect, or group × gain interaction.

Force variability

Figure 3D shows mean force variability for the stroke group and the control group at each gain level for the unimpaired hand. A two-way [group (2) × gain (3)] ANOVA on the unimpaired hand revealed a main effect of gain [$F(1.28,33.37) = 59.94$; $P < 0.01$; $\eta^2 = 0.70$], showing a reduction in variability with an increase in visual gain (low > medium > high). There was no significant effect of group [$F(1,26) = 0.32$; $P = 0.58$], and no group × gain interaction [$F(1.28,33.37) = 0.13$; $P = 0.78$].

Figure 3E shows mean force variability for the stroke group and the control group at each level of visual gain for the impaired hand. Force variability was greater in the stroke group as compared with the control group at all gain levels. Force variability was higher at low visual gain and decreased with increases in visual gain for both groups. The data shown in Figure 3E are consistent with findings from the two-way ANOVA on force variability

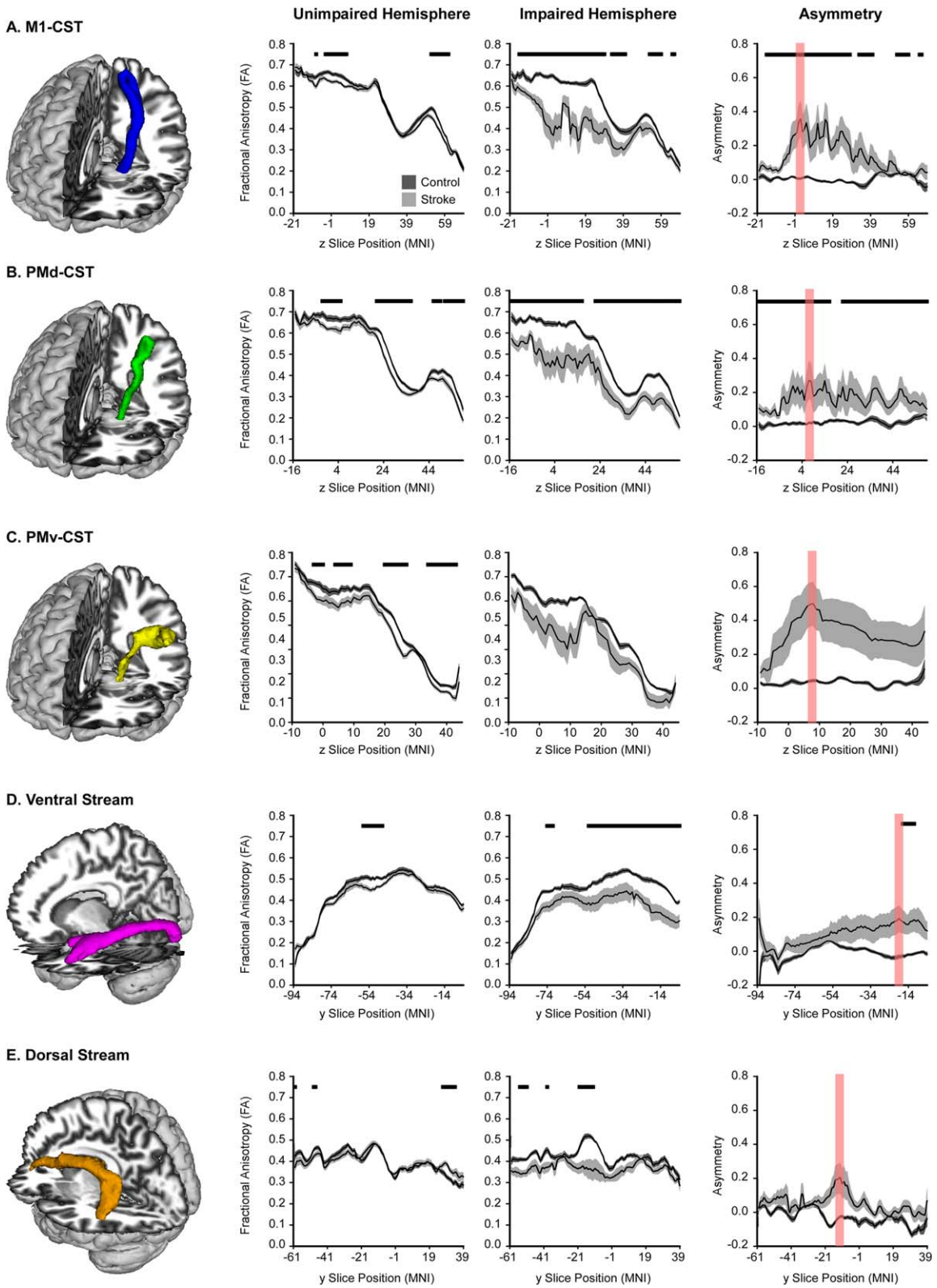

Figure 4.

Probabilistic Tractography in Motor and Visual Tracts. FA profiles of all motor and visual tracts. The mean FA for each group is displayed with a black line, and the dark gray (control) and light gray (stroke) shaded areas represent $\pm$ SEM for each group. Comparisons were made in the unimpaired hemisphere and impaired hemisphere, with FDR corrected $P < 0.05$ represented with horizontal black lines in each plot. Asymmetry of each slice within each tract was also calculated, and is displayed in the final column. The slice with the highest asymmetry is highlighted in red, and represents the region used to extract data for the multiple regression analyses.

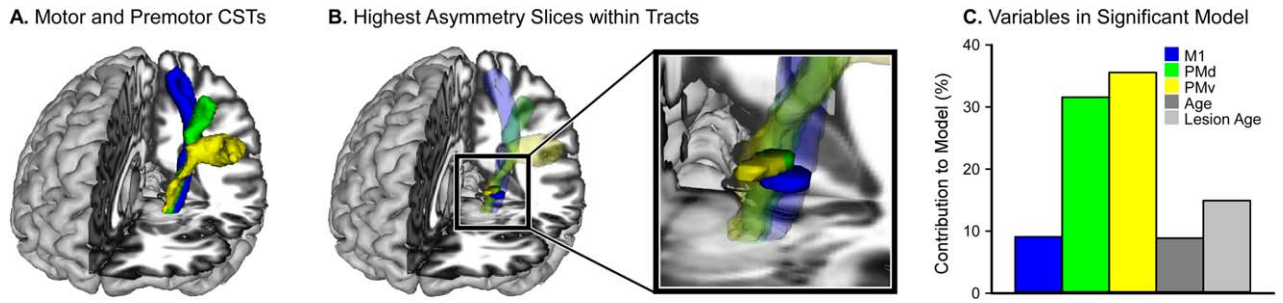

Figure 5.

Contribution to Force Variability. A: The three CST's overlaid on a T1 template (M1 – blue, PMd – green, PMv – yellow). **B**: The largest between group differences in FA asymmetry were found in the PLIC for each motor CST. The black box magnifies the PLIC region of the tract and shows these regions in solid colors superimposed over the corresponding transparent CSTs. **C**: The contribution of each ROI and behavioral variable to the model that best predicted force variability across all levels of the visual gain task.

which revealed significant main effects of group [$F(1,26) = 18.38$; $P < 0.01$; $\eta^2 = 0.41$] and gain [$F(1.13,29.48) = 8.37$; $P < 0.01$; $\eta^2 = 0.24$], but no group × gain interaction [$F(1.13,29.48) = 1.55$; $P = 0.23$]. The stroke group showed increases in variability compared with the control group (see Table II). In the entire cohort, force variability was reduced as visual gain was increased (low > medium > high; all $P < 0.05$, FDR corrected). Figure 3F shows that asymmetry scores for force variability were similar across gain levels within each group, but were lower for the stroke group compared to the control group (Table II). One sample t-tests revealed that asymmetry in the stroke group differed from 0 at the low ($P = 0.01$), medium ($P < 0.001$), and high ($P < 0.001$) gain levels. In contrast, asymmetry in the control group did not differ from 0 at any gain level. These findings demonstrate that stroke-related motor impairment, rather than hand dominance, was the primary factor driving task performance.

MRI Analysis

Probabilistic tractography

Figure 4 shows the probabilistic tractography results for each tract (column 1) and its corresponding slice-by-slice FA profile in the unimpaired hemisphere (column 2), impaired hemisphere (column 3), and asymmetry profile (column 4). Figure 4A shows the conjunction of the tract between the cerebral peduncle and M1 (M1-CST, blue tract). The tract began at $z = -21$ at the level of the cerebral peduncle and terminated at the precentral gyrus at $z = 68$. To characterize the FA within the tract, we first determined the average FA of each slice within the tract for both groups in the unimpaired hemisphere. Data from the stroke group are represented by black lines (average) and light gray shading (±SEM). Data from the control group are represented by black lines and dark gray shading. The tracts showed a similar pattern for each group, with relatively high FA found between the cerebral peduncle and the PLIC ($z = -21$ to $z = 21$). At the level of the centrum semiovale ($z = 21$), FA begins to decrease, consistent with the increased number of crossing fibers in this region. Once the tract leaves the centrum semiovale, there is a relative increase in FA which peaks at $z = 50$, followed by a subsequent decrease where the tract enters gray matter. Comparing groups within the unimpaired hemisphere, there were some significantly different slices in which the stroke group had decreased FA. Significant differences between slices are marked by horizontal black lines above each plot. In the impaired hemisphere, the control group displayed a tract similar to the unimpaired hemisphere, whereas the stroke FA profile was lower and more variable than the control group, especially between $z = -1$ and $z = 19$, which is within the PLIC. Column 4 in Figure 4A shows the FA asymmetry profile for each slice within the M1-CST. The control group had asymmetry near 0 across the entire tract. In contrast, the stroke group had greater tract asymmetry, which was significantly higher than the control group and greatest at the level of the PLIC. The highest value of asymmetry within the tract is shown in red in Figure 4A, and this illustrates the slices within the tract that correspond to the ROI used in the multiple regression analysis. For example, for the M1-CST, the highest asymmetry in the stroke group was located at $z = 1$. Therefore, the ROI was centered a $z = 1$ and a slice superior and inferior were also used within the ROI; thus, the ROI encompassed the M1-CST between $z = 0$ and $z = 2$. This ROI is represented in red in Figure 4A, and an additional illustration of this region is shown in Figure 5B.

The same probabilistic tractography analyses were performed for the other four tracts of interest. These tracts are shown in Figure 4B–E. The tract connecting the cerebral peduncle to PMd (PMd-CST; Fig. 4B, green) followed a similar pattern to the M1-CST. The stroke group had

TABLE III. Multivariate regression coefficients and statistics

	Coefficients						Model Statistics				
Model	Intercept	M1	PMd	PMv	Age	Lesion age	Degrees of freedom	*F*	*P*	Corrected *P*	R^2_{adj}
Overall variability	**−2.07**	**−1.29**	**−3.45**	**4.53**	**0.03**	**−0.04**	**(5,7)**	**20.28**	**0.00**	**0.00**	**88.93**
Low gain variability	−0.54	−0.56	−1.59	2.01	0.01	−0.01	(5,7)	8.27	0.01	0.01	75.18
Medium gain variability	−0.88	−0.76	−0.85	1.55	0.01	−0.01	(5,7)	5.34	0.02	0.03	64.38
High gain variability	−0.65	0.03	−1.01	0.97	0.01	−0.02	(5,7)	4.68	0.03	0.04	60.54

Regression statistics are shown for the best fit multivariate multiple regression model (bolded), as well as the best fit multiple regression model at each gain level for variability.

decreased FA compared to controls within some of the unimpaired hemisphere tract and much of the impaired hemisphere tract. Additionally, the stroke group had greater FA asymmetry across much of the tract, with the highest asymmetry located at $z = 6$ within the PLIC. This slice, in addition to one superior and one inferior slice, was used as an ROI for the multiple regression analysis; thus, the ROI encompassed the PMd-CST between $z = 5$ and $z = 7$. This ROI is shown in red in Figure 4B, and an additional illustration of this ROI is shown in Figure 5B. The tract connecting the cerebral peduncle to PMv (PMv-CST) is shown in Figure 4C in yellow. Within the unimpaired hemisphere, there were some differences between groups in which the stroke group had decreased FA; however, there were no differences in FA in the impaired hemisphere, which could be a result of high tract volume as the tract moves laterally to PMv. Moreover, there were no differences in asymmetry values between groups within this tract. The highest asymmetry within this tract for the stroke group was located at $z = 6$ within the PLIC. This slice, in addition to one superior and one inferior slice, was used as an ROI for the multiple regression analysis; thus, the ROI encompassed the PMv-CST between $z = 5$ and $z = 7$. This ROI is shown in red in Figure 4C, and an additional illustration of this ROI is shown in Figure 5B.

The ventral stream is shown in Figure 4D in magenta, which shows the tract progressing from V1 to the inferior fusiform gyrus. The FA profiles looked similar between groups in the unimpaired hemisphere, with between group differences found in a small section of the tract between $y = -48$ and $y = -58$, which corresponds with the middle temporal gyrus. Between group differences were more pronounced in the impaired hemisphere, with the stroke group showing reduced FA across much of the tract. However, negligible between group differences were found in FA asymmetry scores, with significant differences only found in the most anterior portions of the tract. The highest asymmetry score in the stroke group was found at $y = -20$ within the fusiform gyrus. Finally, the dorsal stream is shown in Figure 4E in orange and extends from V3 to the inferior frontal gyrus. Extensive between group differences in the dorsal stream were not evidenced in either the impaired or unimpaired hemisphere and this was ultimately reflected in nonsignificant between group asymmetry findings. The highest asymmetry value within the stroke group was located at $y = -16$ within the precentral gyrus.

Multiple regression

The slices demonstrating the largest asymmetry within each tract (shown in red, Fig. 4) were used to position an ROI from which FA asymmetry values were calculated for each individual. As an example, Figure 5A displays the three motor tracts, and 5B displays the portions of the tract containing the highest asymmetry values. FA asymmetry values were used in a multivariate multiple regression analysis, which was conducted with bidirectional elimination, to determine which tracts describe the variance in force variability within the visual gain task. For this analysis, FA asymmetry in M1, PMd, PMv, and ventral and dorsal ROIs were used as independent variables. Age, lesion age, lesion size, and UE FMA were also entered into the model as behavioral independent variables. Dependent variables were low, medium, and high force variability. The final model contained FA asymmetry in M1, PMd, and PMv ROIs, as well as age and lesion age. Together these variables predicted 88.9% of the variance in force variability ($P = 0.01$). The overall contribution of each region (M1 = 9.08%, PMd = 31.58%, PMv = 35.56%, Age = 14.92%, Lesion Age = 8.86%) is shown in Figure 5C. Model coefficients and other statistics are shown in Table III. Note that the ventral and dorsal visual tracts did not contribute to the model that best predicted force variability. This finding highlights the specificity of our findings in primary and premotor CSTs.

Separate follow-up multiple regression analyses were then conducted for low, medium, and high force variability using the independent variables identified in the multivariate multiple regression. Significant FDR corrected models were found for force variability at each gain level (Low: $R^2_{adj} = 75.18$, $P = 0.01$; Medium: $R^2_{adj} = 64.38$, $P = 0.03$; High: $R^2_{adj} = 60.54$, $P = 0.04$). We found that PMd and PMv contributed most to the model that best predicted force variability, while M1, age, and lesion age contributed

much less. At the low level of visual gain, PMd contributed 43% and PMv contributed 39%. The remaining independent variables contributed between 2 and 9%. At the medium level of visual gain, PMd contributed 13% and PMv contributed 32%. The remaining independent variables contributed between 0 and 24%. At the high level of visual gain, PMd contributed 37% and PMv contributed 23%. The remaining independent variables contributed between 2 and 18% across all gain levels.

Secondary control analyses were completed to determine if lesion load within M1, PMd, or PMv was predictive of force variability at each gain level. Lesion load was calculated by overlaying each individual's lesion map with M1, PMd, and PMv regions of the Human Motor Area Template [Mayka et al., 2006], and counting the number of overlapping voxels within each region. Lesion load for M1, PMd, and PMv, as well as age, lesion age, lesion size, and UE FMA were all entered into a multivariate model. There were no significant models, indicating that lesion load of M1, PMd, and PMv were not significant predictors of force variability at any gain level.

DISCUSSION

This study examined the relationship between force variability during a visuomotor force task at three levels of visual gain and microstructural properties of motor, premotor, and visual tracts in poststroke individuals. First, we found that individuals poststroke reduced force variability with an increase in visual gain, despite extensive microstructural damage in the primary motor CST, premotor CSTs, and visual tracts. Second, microstructure in primary motor and premotor CSTs predicted force variability across all gain levels, whereas microstructure of visual tracts did not. Third, CSTs projecting from the premotor cortex, as compared with the primary motor cortex, contributed the greatest amount to the model that best predicted force variability in poststroke individuals. These findings provide novel evidence that the segregation of the CST into motor and premotor components can be a useful tool in the prediction of visuomotor processing in poststroke individuals.

Increases in Visual Gain Lead to Decreases in Force Variability

Between group differences in force variability revealed that individuals poststroke had higher force variability as compared with controls. It is important to note that both groups reduced force variability with an increase in visual gain, and that changes in variability were not driven by changes in mean force, as mean force did not vary as a function of group or gain level. Demonstrating that alterations in visual gain can influence motor task performance is consistent with previous studies in chronic stroke that have manipulated visual feedback to alter force amplitude and range of motion [Brewer et al., 2005, 2008], joint excursion and trajectory smoothness of finger movements, and CST excitability [Bagce et al., 2012]. Improvement in the movement trajectory produced by individuals poststroke has also been shown following training paradigms with forces that amplify movement error [Patton et al., 2006]. Combining visual and haptic distortions to amplify upper-extremity tracking error by a factor of 1.5 has also been found to reduce motor impairment and improve motor function following a two week treatment intervention in a cohort of chronic stroke patients [Abdollahi et al., 2013]. However, since both visual and haptic distortions were used, it is unclear if visual distortion alone can lead to alterations in force production in poststroke individuals. In this study, we provide evidence that manipulating the properties of visual feedback alone attenuates variability during a visuomotor force task.

Reducing performance error is a basic principle of motor learning, and learning progresses more quickly when errors are large [Rumelhart et al., 1988]. In the presence of errors, the sensorimotor control system engages visuomotor feedback pathways to process this information until the feedforward controller learns the appropriate dynamics [Franklin et al., 2012]. Given the continuous characteristic of the force control task we used here, it is difficult to differentiate feedforward and feedback control, although previous neuroimaging findings suggest that increases in visual gain more strongly engage a feedback control network that includes premotor cortex, inferior parietal cortex, and extrastriate visual cortex as compared to the cerebellar circuits that are implicated in feedforward control [Bastian, 2006; Coombes et al., 2010; Therrien and Bastian, 2015; Vaillancourt et al., 2006b]. Augmented error has been studied in the context of motor learning using force field adaptation and perturbation paradigms during upper and lower limb tasks [Emken and Reinkensmeyer, 2005; Patton et al., 2013]. Although these findings do not inform learning models associated with error augmentation directly, they demonstrate that changes in visual gain during a continuous force control task can be used to drive acute changes in force variability, even following stroke.

Tract Specific Microstructure Predicts Force Variability in Individuals Poststroke

The multivariate multiple regression analysis revealed an association between grip force variability and FA in primary motor and premotor CSTs. This finding is consistent with evidence that the microstructural properties of the primary motor and premotor CSTs predict upper-extremity function in individuals poststroke [Bagce et al., 2012; Perez and Cohen, 2009; Schulz et al., 2012; Stinear et al., 2007], and with evidence that FA in the PLIC correlates positively with motor skill and grip strength in individuals poststroke [Lindenberg et al., 2010; Schaechter et al., 2008]. While our data support the notion that the FA of the primary motor CST is associated with upper-

extremity visuomotor processing, we found that its contribution to the model that best predicted force variability was 9%, while the contribution of premotor CST microstructure contributed 66%. Hence, the novel finding of this study is that microstructure in the premotor CSTs most strongly predicted visual gain-induced changes in force variability in individuals poststroke. The role of premotor cortex function for visuomotor processing and the impact of stroke on premotor cortex function are two possible explanations for our findings.

Role of Premotor Cortex in Visuomotor Processing

The association between grip force variability and FA in the premotor CST links well with evidence that PMd and PMv are involved in visuomotor processing. Both PMd and PMv are key components of the visuomotor network, and PMd, in particular, has been consistently identified in neuroimaging studies that assess visuomotor processing and feedback control [Coombes et al., 2010; Vaillancourt et al., 2006b]. In nonhuman primates, neural activity in PMd increases during spatial cues that instruct direction specific motor responses [di Pellegrino and Wise, 1993; Weinrich and Wise, 1982]. In humans, studies show that the BOLD signal in PMd scales with force amplitude when an individual is guided by visual cues [Chouinard et al., 2005], and TMS-elicited virtual lesions disrupt PMd function and lead to errors in visuomotor control [Davare et al., 2006]. PMv is also important for visuomotor processing, is a critical part of the grasping network, and controls the preshaping of the hand to objects [Kantak et al., 2012]. Inactivation of PMv in nonhuman primates results in inaccurate preshaping of the hand [Fogassi et al., 2001], and TMS over PMv in humans disrupts finger position on an object [Davare et al., 2006]. These studies suggest that PMd and PMv play a pivotal role in the integration of visual information into motor commands and grasping objects.

Using a similar visual gain paradigm to that used in this study, we have previously shown that acute changes in visual gain alter functional activity in the visuomotor network in healthy adults, including M1, PMd, and PMv [Coombes et al., 2010]. Small increases in visual gain were associated with acute increases in functional activity within M1, and were accompanied by a significant reduction in force error. In contrast, large increases in functional activity within PMd were only evident with large changes in visual gain from moderate to high visual gain levels; PMv, however, exhibited large changes in functional activity with both small and large changes in visual gain. This finding demonstrated that acute changes in visual gain correspond with acute changes in brain activity in the cortical motor system. In this study, we extend these findings by associating brain structure in key visuomotor pathways with performance in a visual gain task in the chronic phase after stroke. This is a key advance in the literature because we show for the first time that visuomotor processing can be predicted by a relatively stable measurement of brain microstructure in specific CSTs.

Role of Premotor Cortex in the Chronic Phase after Stroke

Lesions that directly impact M1 are common because M1 is intricately connected to branches of the middle cerebral artery [Cramer et al., 2000]. Following damage to the primary motor CST, the central nervous system takes advantage of alternate premotor pathways to control upper-extremity movement [Dum and Strick, 1991; Plow et al., 2015]. For instance, injecting muscimol into PMd in the lesioned hemisphere in nonhuman primates inhibits recovery from weakness following a focal experimental lesion in M1 [Fridman et al., 2004; Liu and Rouiller, 1999], and human stimulation studies have consistently linked premotor cortex activation with the trajectory of stroke recovery [Fridman et al., 2004; Johansen-Berg et al., 2002; Plow et al., 2015]. These and other findings have led Kantak et al. [2012] to propose the premotor reorganization hypothesis, which suggests that lesion load of the primary motor CST influences the extent to which premotor cortex is engaged during voluntary movement. Much of the evidence supporting a role for premotor cortex comes from functional neuroimaging studies and TMS studies [Johansen-Berg et al., 2002; Kang and Cauraugh, 2015; O'Shea et al., 2007; Plow et al., 2015; Ward et al., 2006], although evidence has identified a significant relationship between microstructural properties of the premotor CST and grip force strength [Newton et al., 2006; Schulz et al., 2012], Here, we compliment these findings to show that FA asymmetry of the premotor CST predicts force variability during a visuomotor task.

Predicting motor function and motor recovery with measures of brain microstructure is attractive because diffusion MRI scans are task and severity independent, meaning that stroke severity is not a limiting factor for data collection. Methodological advances over the last decade have improved our ability to identify specific tracts in the brain. For instance, previous studies have used hand drawn ROI analyses to characterize the association between FA in the PLIC with motor control and recovery in individuals poststroke [Park et al., 2013; Stinear et al., 2007], but these hand drawn ROIs likely included portions of the primary motor and premotor CST. Other studies have used tractography algorithms to calculate mean FA in the entire CST, but these studies have either restricted the tracking algorithm to the primary motor CST, [Lindenberg et al., 2012; Park et al., 2013; Schaechter et al., 2009], or when also tracking from premotor areas, have only examined the relation between entire tract FA and grip strength [Schulz et al., 2012]. Here, we used a novel approach where we first used probabilistic tractography algorithms in controls to identify the CST projecting from

M1, PMd, and PMv. We then used this template to analyze FA of each slice within each tract for both control and stroke subjects. Next, we selected ROIs based on slices within each tract that exhibited the highest asymmetry in the stroke subjects. Highest asymmetry in each motor and premotor CST was located within the PLIC, which corroborates previous evidence that PLIC microstructure predicts upper-extremity function after stroke [Park et al., 2013; Stinear et al., 2007]. However, our observation that premotor PLIC microstructure contributed more to the prediction of force variability in poststroke individuals as compared with regions of the PLIC associated with the primary motor CST demonstrates the importance of segregating PLIC regions by seeding distinct cortical motor areas. Our findings suggest that microstructure of premotor CSTs may be helpful in predicting intervention outcomes associated with visuomotor paradigms for stroke motor recovery [Abdollahi et al., 2013; Patton et al., 2006].

Four alternative explanations can be offered for our findings. First, although we screened for intact sensation to light touch and proprioception in the impaired arm/hand, we did not perform detailed sensory discrimination testing nor screen for sensory deficits specific to the task. However, the task was designed to drive feedback control rather than feedforward control and proprioception. Second, our groups were predominantly male. Sex differences are an unlikely explanation for our findings, however, because force amplitude was normalized across all subjects, and stroke and control groups were well matched for sex. Hand dominance is a third potential explanation for our findings, but symmetry in force variability scores in controls and asymmetric force variability scores in the stroke group suggest that motor impairment, rather than hand dominance, was the primary factor driving differences in task performance following stroke. Fourth, hemispheric laterality of stroke is an important variable when examining motor function after stroke [Schaefer et al., 2012]. Although stroke laterality was not controlled in this study, regardless of group all subjects showed reductions in force variability with increases in visual gain. Moreover, laterality data showed that task performance in controls was not sensitive to differences in hemispheric specialization for motor control.

CONCLUSIONS

Individuals poststroke reduced force variability as visual gain levels increased despite widespread microstructural deficits in motor and visual tracts. FA within the descending motor pathways predicted force variability in poststroke individuals, with premotor areas (PMd and PMv) of PLIC contributing more than the primary motor (M1) area of PLIC, to the statistical model that best predicted force variability. Although our findings are limited to the prediction of acute changes in force variability via changes in visual feedback, they provide a foundation for future studies to explore the role of premotor CSTs in visuomotor processing.

ACKNOWLEDGMENT

MRI data collection was supported through the National High Magnetic Field Laboratory and obtained at the Advanced Magnetic Resonance Imaging and Spectroscopy facility in the McKnight Brain Institute of the University of Florida.

REFERENCES

Abdollahi F, Case Lazarro ED, Listenberger M, Kenyon RV, Kovic M, Bogey RA, Hedeker D, Jovanovic BD, Patton JL (2013): Error Augmentation Enhancing Arm Recovery in Individuals With Chronic Stroke: A Randomized Crossover Design. Neurorehabil Neural Repair 28:120–128.

Bagce HF, Saleh S, Adamovich SV, Tunik E (2012): Visuomotor gain distortion alters online motor performance and enhances primary motor cortex excitability in patients with stroke. Neuromodulation 15:361–366.

Bastian AJ (2006): Learning to predict the future: the cerebellum adapts feedforward movement control. Curr Opin Neurobiol 16:645–649.

Bohannon RW, Smith MB (1987): Interrater reliability of a modified Ashworth scale of muscle spasticity. Phys Ther 67: 206–207.

Brewer BR, Fagan M, Klatzky RL, Matsuoka Y (2005): Perceptual limits for a robotic rehabilitation environment using visual feedback distortion. IEEE Trans Neural Syst Rehabil Eng 13:1–11.

Brewer BR, Klatzky R, Matsuoka Y (2008): Visual feedback distortion in a robotic environment for hand rehabilitation. Brain Res Bull 75:804–813.

Caeyenberghs K, Leemans A, Geurts M, Taymans T, Linden CV, Smits-Engelsman BCM, Sunaert S, Swinnen SP (2010): Brain-behavior relationships in young traumatic brain injury patients: Fractional anisotropy measures are highly correlated with dynamic visuomotor tracking performance. Neuropsychologia 48:1472–1482.

Chouinard PA, Leonard G, Paus T (2005): Role of the primary motor and dorsal premotor cortices in the anticipation of forces during object lifting. J Neurosci 25:2277–2284.

Clas P, Groeschel S, Wilke M (2012): A semi-automatic algorithm for determining the demyelination load in metachromatic leukodystrophy. Acad Radiol 19:26–34.

Coombes SA, Corcos DM, Sprute L, Vaillancourt DE (2010): Selective regions of the visuomotor system are related to gain-induced changes in force error. J Neurophysiol 103:2114–2123.

Coombes SA, Corcos DM, Vaillancourt DE (2011): Spatiotemporal tuning of brain activity and force performance. Neuroimage 54:2226–2236.

Cramer SC, Moore CI, Finklestein SP, Rosen BR (2000): A pilot study of somatotopic mapping after cortical infarct. Stroke 31: 668–671.

Davare M, Andres M, Cosnard G, Thonnard JL, Olivier E (2006): Dissociating the role of ventral and dorsal premotor cortex in precision grasping. J Neurosci 26:2260–2268.

de Haan B, Clas P, Juenger H, Wilke M, Karnath HO (2015): Fast semi-automated lesion demarcation in stroke. Neuroimage Clin 9:69–74.

di Pellegrino G, Wise SP (1993): Visuospatial versus visuomotor activity in the premotor and prefrontal cortex of a primate. J Neurosci 13:1227–1243.

Dum RP, Strick PL (1991): The origin of corticospinal projections from the premotor areas in the frontal lobe. J Neurosci 11:667–689.

Emken JL, Reinkensmeyer DJ (2005): Robot-enhanced motor learning: accelerating internal model formation during locomotion by transient dynamic amplification. IEEE Trans Neural Syst Rehabil Eng 13:33–39.

Fogassi L, Gallese V, Buccino G, Craighero L, Fadiga L, Rizzolatti G (2001): Cortical mechanism for the visual guidance of hand grasping movements in the monkey: A reversible inactivation study. Brain 124:571–586.

Folstein MF, Folstein SE, McHugh PR (1975): "Mini-mental state". A practical method for grading the cognitive state of patients for the clinician. J Psychiatr Res 12:189–198.

Franklin S, Wolpert DM, Franklin DW (2012): Visuomotor feedback gains upregulate during the learning of novel dynamics. J Neurophysiol 108:467–478.

Fridman EA, Hanakawa T, Chung M, Hummel F, Leiguarda RC, Cohen LG (2004): Reorganization of the human ipsilesional premotor cortex after stroke. Brain 127:747–758.

Fugl-Meyer AR, Jaasko L, Leyman I, Olsson S, Steglind S (1975): The post-stroke hemiplegic patient. 1. A method for evaluation of physical performance. Scand J Rehabil Med 7:13–31.

Gladstone DJ, Danells CJ, Black SE (2002): The fugl-meyer assessment of motor recovery after stroke: A critical review of its measurement properties. Neurorehabil Neural Repair 16: 232–240.

Gromping U (2006): Relative importance for linear regression in R: The package relaimpo. J Stat Software 17:1–27.

Haar S, Donchin O, Dinstein I (2015): Dissociating visual and motor directional selectivity using visuomotor adaptation. J Neurosci 35:6813–6821.

Haas BM, Bergstrom E, Jamous A, Bennie A (1996): The inter rater reliability of the original and of the modified Ashworth scale for the assessment of spasticity in patients with spinal cord injury. Spinal Cord 34:560–564.

Hoshi E, Tanji J (2000): Integration of target and body-part information in the premotor cortex when planning action. Nature 408:466–470.

Jager HR (2005): Loss of vision: Imaging the visual pathways. Eur Radiol 15:501–510.

Jenkinson M, Smith S (2001): A global optimisation method for robust affine registration of brain images. Med Image Anal 5: 143–156.

Jenkinson M, Bannister P, Brady M, Smith S (2002): Improved optimization for the robust and accurate linear registration and motion correction of brain images. Neuroimage 17:825–841.

Jenkinson M, Beckmann CF, Behrens TE, Woolrich MW, Smith SM (2012): Fsl. Neuroimage 62:782–790.

Johansen-Berg H, Rushworth MF, Bogdanovic MD, Kischka U, Wimalaratna S, Matthews PM (2002): The role of ipsilateral premotor cortex in hand movement after stroke. Proc Natl Acad Sci USA 99:14518–14523.

Kang N, Cauraugh JH (2015): Force control in chronic stroke. Neurosci Biobehav Rev 52:38–48.

Kantak SS, Stinear JW, Buch ER, Cohen LG (2012): Rewiring the brain: Potential role of the premotor cortex in motor control, learning, and recovery of function following brain injury. Neurorehabil Neural Repair 26:282–292.

Krebs HI, Brashers-Krug T, Rauch SL, Savage CR, Hogan N, Rubin RH, Fischman AJ, Alpert NM (1998): Robot-aided functional imaging: Application to a motor learning study. Hum Brain Mapp 6:59–72.

Laidlaw DH, Bilodeau M, Enoka RM (2000): Steadiness is reduced and motor unit discharge is more variable in old adults. Muscle Nerve 23:600–612.

Lee Hong S, Newell KM (2008): Visual information gain and the regulation of constant force levels. Exp Brain Res 189:61–69.

Lindenberg R, Renga V, Zhu LL, Betzler F, Alsop D, Schlaug G (2010): Structural integrity of corticospinal motor fibers predicts motor impairment in chronic stroke. Neurology 74:280–287.

Lindenberg R, Zhu LL, Ruber T, Schlaug G (2012): Predicting functional motor potential in chronic stroke patients using diffusion tensor imaging. Hum Brain Mapp 33:1040–1051.

Liu Y, Rouiller EM (1999): Mechanisms of recovery of dexterity following unilateral lesion of the sensorimotor cortex in adult monkeys. Exp Brain Res 128:149–159.

Lodha N, Coombes SA, Cauraugh JH (2012a): Bimanual isometric force control: Asymmetry and coordination evidence post stroke. Clin Neurophysiol 123:787–795.

Lodha N, Patten C, Coombes SA, Cauraugh JH (2012b): Bimanual force control strategies in chronic stroke: Finger extension versus power grip. Neuropsychologia 50:2536–2545.

Mayka MA, Corcos DM, Leurgans SE, Vaillancourt DE (2006): Three-dimensional locations and boundaries of motor and premotor cortices as defined by functional brain imaging: A meta-analysis. Neuroimage 31:1453–1474.

Mochizuki H, Franca M, Huang YZ, Rothwell JC (2005): The role of dorsal premotor area in reaction task: Comparing the "virtual lesion" effect of paired pulse or theta burst transcranial magnetic stimulation. Exp Brain Res 167:414–421.

Naik SK, Patten C, Lodha N, Coombes SA, Cauraugh JH (2011): Force control deficits in chronic stroke: Grip formation and release phases. Exp Brain Res 211:1–15.

Newell KM, McDonald PV (1994): Information, coordination modes and control in a prehensile force task. Hum Movement Sci 13:375–391.

Newton JM, Ward NS, Parker GJ, Deichmann R, Alexander DC, Friston KJ, Frackowiak RS (2006): Non-invasive mapping of corticofugal fibres from multiple motor areas–relevance to stroke recovery. Brain 129:1844–1858.

O'Shea J, Johansen-Berg H, Trief D, Gobel S, Rushworth MF (2007): Functionally specific reorganization in human premotor cortex. Neuron 54:479–490.

Oldfield RC (1971): The assessment and analysis of handedness: The Edinburgh inventory. Neuropsychologia 9:97–113.

Park CH, Kou N, Boudrias MH, Playford ED, Ward NS (2013): Assessing a standardised approach to measuring corticospinal integrity after stroke with DTI. Neuroimage Clin 2:521–533.

Patten C, Condliffe EG, Dairaghi CA, Lum PS (2013): Concurrent neuromechanical and functional gains following upper-extremity power training post-stroke. J Neuroeng Rehabil 10:1

Patton JL, Stoykov ME, Kovic M, Mussa-Ivaldi FA (2006): Evaluation of robotic training forces that either enhance or reduce error in chronic hemiparetic stroke survivors. Exp Brain Res 168:368–383.

Patton JL, Wei YJ, Bajaj P, Scheidt RA (2013): Visuomotor learning enhanced by augmenting instantaneous trajectory error feedback during reaching. PloS One 8:e46466

Perez MA, Cohen LG (2009): The corticospinal system and transcranial magnetic stimulation in stroke. Top Stroke Rehabil 16: 254–269.

Plow EB, Cunningham DA, Varnerin N, Machado A (2015): Rethinking stimulation of the brain in stroke rehabilitation: Why higher motor areas might be better alternatives for patients with greater impairments. Neuroscientist 21:225–240.

Rumelhart DE, Hinton GE, Williams RJ (1988): Learning representations by back-propagating errors. Cogn Model 5:3.

Schaechter JD, Perdue KL, Wang R (2008): Structural damage to the corticospinal tract correlates with bilateral sensorimotor cortex reorganization in stroke patients. Neuroimage 39:1370–1382.

Schaechter JD, Fricker ZP, Perdue KL, Helmer KG, Vangel MG, Greve DN, Makris N (2009): Microstructural status of ipsilesional and contralesional corticospinal tract correlates with motor skill in chronic stroke patients. Hum Brain Mapp 30: 3461–3474.

Schaefer SY, Mutha PK, Haaland KY, Sainburg RL (2012): Hemispheric specialization for movement control produces dissociable differences in online corrections after stroke. Cerebral Cortex 22:1407–1419.

Schluter ND, Rushworth MF, Passingham RE, Mills KR (1998): Temporary interference in human lateral premotor cortex suggests dominance for the selection of movements. A study using transcranial magnetic stimulation. Brain 121:785–799.

Schulz R, Park CH, Boudrias MH, Gerloff C, Hummel FC, Ward NS (2012): Assessing the integrity of corticospinal pathways from primary and secondary cortical motor areas after stroke. Stroke 43:2248–2251.

Slifkin AB, Newell KM (1999): Noise, information transmission, and force variability. J Exp Psychol Hum Percept Perform 25: 837–851.

Smith SM (2002): Fast robust automated brain extraction. Hum Brain Mapp 17:143–155.

Smith SM, Jenkinson M, Woolrich MW, Beckmann CF, Behrens TE, Johansen-Berg H, Bannister PR, De Luca M, Drobnjak I, Flitney DE, et al. (2004): Advances in functional and structural MR image analysis and implementation as FSL. Neuroimage 23:S208–S219.

Stinear CM, Barber PA, Smale PR, Coxon JP, Fleming MK, Byblow WD (2007): Functional potential in chronic stroke patients depends on corticospinal tract integrity. Brain 130: 170–180.

Therrien AS, Bastian AJ (2015): Cerebellar damage impairs internal predictions for sensory and motor function. Curr Opin Neurobiol 33:127–133.

Vaillancourt DE, Haibach PS, Newell KM (2006a): Visual angle is the critical variable mediating gain-related effects in manual control. Exp Brain Res 173:742–750.

Vaillancourt DE, Mayka MA, Corcos DM (2006b): Intermittent visuomotor processing in the human cerebellum, parietal cortex, and premotor cortex. J Neurophysiol 95:922–931.

Volpe BT, Krebs HI, Hogan N, Edelstein OL, Diels C, Aisen M (2000): A novel approach to stroke rehabilitation: Robot-aided sensorimotor stimulation. Neurology 54:1938–1944.

Wang LE, Tittgemeyer M, Imperati D, Diekhoff S, Ameli M, Fink GR, Grefkes C (2012): Degeneration of corpus callosum and recovery of motor function after stroke: A multimodal magnetic resonance imaging study. Hum Brain Mapp 33:2941–2956.

Ward NS, Newton JM, Swayne OB, Lee L, Thompson AJ, Greenwood RJ, Rothwell JC, Frackowiak RS (2006): Motor system activation after subcortical stroke depends on corticospinal system integrity. Brain 129:809–819.

Weinrich M, Wise SP (1982): The premotor cortex of the monkey. J Neurosci 2:1329–1345.

Wilke M, de Haan B, Juenger H, Karnath HO (2011): Manual, semi-automated, and automated delineation of chronic brain lesions: A comparison of methods. Neuroimage 56:2038–2046.

Wolter M, Preda S (2006): Visual deficits following stroke: Maximizing participation in rehabilitation. Top Stroke Rehabil 13: 12–21.

Woolrich MW, Jbabdi S, Patenaude B, Chappell M, Makni S, Behrens T, Beckmann C, Jenkinson M, Smith SM (2009): Bayesian analysis of neuroimaging data in FSL. Neuroimage 45: S173–S186.

Yoshida S, Hayakawa K, Yamamoto A, Okano S, Kanda T, Yamori Y, Yoshida N, Hirota H (2010): Quantitative diffusion tensor tractography of the motor and sensory tract in children with cerebral palsy. Dev Med Child Neurol 52:935–940.